Three-electron atoms and ions in a magnetic field

J. A. Salas, I. Pelaschier, and K. Varga
Department of Physics and Astronomy, Vanderbilt University, Nashville, Tennessee 37235, USA
(Received 7 August 2015; published 2 September 2015)

The energies and physical properties of three-electron systems are studied using an explicitly correlated Gaussian basis optimized by the stochastic variational method. The stability of the system as a function of the nuclear charge is analyzed. The role of the Coulomb and magnetic interactions in shaping the structure of these systems is discussed. The accuracy of the energies is substantially improved for high magnetic fields.

DOI: 10.1103/PhysRevA.92.033401 PACS number(s): 32.10.Ee

I. INTRODUCTION

The competition between the Coulomb (electron-electron repulsion and electron-nuclear attraction) and the magnetic field for different interaction strengths makes the atoms in the magnetic field a perfect laboratory to test and develop computational approaches [1–12]. In this paper we study the energy levels, wave functions, and structures of three-electron systems as a function of strength of the magnetic and the Coulomb interactions using an accurate variational description.

The study of the effect of magnetic fields on energy levels and wave functions is strongly motivated by the discovery of stars with strong magnetic fields [13–15]. These magnetic field strengths range from the weaker fields of white dwarfs [16,17] ($\approx 10^7$ G) through neutron stars [18] ($\approx 10^{12}$ G) all the way up to fields of 10^{14}–10^{15} G observed in magnetars [19]. Under normal laboratory conditions the highest achievable magnetic field is around 10^5 G, but in condensed-matter systems the low effective mass and high dielectric constant can lead to magnetic fields [20] that are, in effect, much stronger than that.

Many different approaches [21–29] have been used to study the effects of strong magnetic fields on small atoms and ions, such as H, H^-, He, Li, and Be. The most popular approaches include the Hartree-Fock method [1,10,30–39]; variational calculations with Gaussian [2,3], Hylleraas [4,5], or Lagrange basis functions [6]; quantum Monte Carlo (QMC) [7,8], finite-element calculations [9]; and the pseudospectral Hartree-Fock method [10]. Analytical calculations have also been proven to be valuable tools. It has been analytically predicted, for example, that under very strong magnetic fields neutral atoms can bind with an additional electron [11,12]. In particular, it was claimed that helium, despite being a noble gas, was capable of forming a stable negative ion under such conditions. Recent works based on computational methods have verified this prediction of the He^- ion [5,40].

While many papers in the literature deal with two-electron atoms [2–4,6–9], accurate calculations for three or more electrons are rare. Computational studies of Li, as well as He^- and Be^+ ions, are mostly done by using methods based on some simplifying approximations [5,35,36,41–46], for example, by using the Hartree-Fock method [1,10,30–39] or methods that restrict the core electrons [47,48]. For three-electron atoms the configuration interaction method with anisotropic Gaussian basis functions [1] and Hylleraas basis functions [4] seems to give accurate results.

The effect of magnetic field on the energy levels of molecules has also been extensively studied [49–58]. High magnetic fields drastically change the binding energies and bond lengths [58] and can lead to new bonding mechanisms [52]. Calculations for molecules are very difficult because the separation of center-of-mass motion [59] is not trivial and the description of nuclear and electronic structure is complicated. Recent works [49,50,53] using current density-functional theory [60] established a nonperturbative framework to calculate the molecular properties in magnetic fields.

Approaches based on explicitly correlated wave functions [4,6,40] are likely to be restricted to smaller atoms, with the only exception being the QMC method [7,8,61]. Beyond few-electron systems, besides the QMC method [7,8], the Hartree-Fock [1,10,30–39] and the density-functional-theory (DFT) approaches [62,63] seem to be applicable. The DFT approaches are particularly important because they can help the development of better exchange-correlational functionals. A recent thorough review of different approaches can be found in Ref. [64].

In this work we extend out previous accurate variational calculations [40] to study the three-electron isoelectronic sequence, with $Z = \{1,2,3,4\}$, in a strong uniform magnetic field. Besides calculating the energy levels, we also analyze the change of the wave functions and make comparisons between the different systems. All this is done within the nonrelativistic framework, neglecting any QED effects and assuming an infinitely massive nucleus, as is commonly done in the literature. The calculations employ a deformed explicitly correlated Gaussian (ECG), and the nonlinear parameters are optimized with the stochastic variational method. Variational calculations using explicitly correlated Gaussians proved to be extremely accurate in predicting binding energies and other properties in few-particle systems including the stability domains [2,65,66]. The main advantage of the ECG basis is that the matrix elements are analytically available, and by increasing the number of basis states the accuracy can be enhanced. In our previous paper [40] we have shown that the deformed variant of this basis is flexible enough to give accurate results for high magnetic fields.

II. FORMALISM

A. Hamiltonian and basis functions

The nonrelativistic Hamiltonian of a Coulombic few-particle system in magnetic field B, oriented in the z direction, is given by

$$H = T + V_{ho} + V_{Ne} + V_{ee} + \frac{B}{2}(L_z + 2S_z) \qquad (1)$$

$$= \sum_{i=1}^{N} \left(-\frac{1}{2}\Delta_i + \frac{B^2}{8}\left(x_i^2 + y_i^2\right) - \frac{Z}{r_i} \right) + \sum_{i<j}^{N} \frac{1}{r_{ij}} + \frac{B}{2}(L_z + 2S_z). \quad (2)$$

Here T is the kinetic energy, V_{ho} is the harmonic oscillator potential, V_{Ne} is the attraction of the nucleus, and V_{ee} is the electron repulsion, with L_z and S_z being, respectively, the angular momentum and total spin operators in the z direction, which correspond to conserved quantities in the system.

We also define V_{mag} as the total contribution of the energy due to the magnetic field:

$$V_{\text{mag}} = \sum_{i=1}^{N} \frac{B^2}{8}\left(x_i^2 + y_i^2\right) + \frac{B}{2}(L_z + 2S_z). \quad (3)$$

The variational method is used to calculate the energy of the system. As a trial function we choose a deformed form of the correlated Gaussians (DCG) [2,3]:

$$\exp\left\{ -\frac{1}{2}\sum_{i,j=1}^{N} A_{ij}\rho_i\rho_j - \frac{1}{2}\sum_{i,j=1}^{N} B_{ij} z_i z_j \right\}, \quad (4)$$

where the nonlinear parameters are different and independent in both the radial and vertical directions.

The Hamiltonian does not commute with L^2, but it has eigenfunctions in common with L_z, with corresponding eigenvalue M. The above form of the DCG belongs to $M = 0$. To allow for $M \neq 0$ states we multiply the basis by

$$\prod_{i=1}^{N} \xi_{m_i}(\rho_i), \quad (5)$$

where

$$\xi_m(\rho) = (x + iy)^m. \quad (6)$$

Thus the spatial antisymmetric variational trial function reads

$$\Phi_M(\mathbf{r}) = \mathcal{A}\left\{ \left(\prod_{i=1}^{N} \xi_{m_i}(\rho_i) \right) \times \exp\left\{ -\frac{1}{2}\sum_{i,j=1}^{N} A_{ij}\rho_i\rho_j - \frac{1}{2}\sum_{i,j=1}^{N} B_{ij} z_i z_j \right\} \right\}, \quad (7)$$

where $M = m_1 + m_2 + \cdots + m_N$ and m_i are integers. This function is coupled with the spin function χ_{SM_S} to form the trial function. The nonlinear parameters are optimized with the stochastic variational method [2,3].

The explicitly correlated Gaussians are very popular in atomic physics and quantum chemistry [2]. The main advantages of ECG bases are (1) their matrix elements are analytically available for a general N-particle system, (2) they are flexible enough to approximate rapidly changing functions, (3) the permutation symmetry can be easily imposed, and (4) one can make a simple transformation between single-particle and relative coordinate systems. The basis parameters can be efficiently chosen by the stochastic variational method [3]. The present basis is restricted to a single center, and the calculations are limited to a single nucleus. One can, in principle, generalize the approach for molecular calculations using multicenter Gaussians [2], but due care has to be taken in treating the center-of-mass motion [59].

B. Threshold energy

In order to determine the stability of the system, one has to calculate the accurate threshold energies. This is done by calculating the energies of the two-electron isoelectronic series in the appropriate configurations. For example, for He^- the threshold is given by the states of He that satisfy the following:

$$E_T(M, S_z) = \min_{M^{He}, S_z^{He}} \left[E_{\text{tot}}^{He}\left(M^{He}, S_z^{He}\right) + E^e\left(M^e, S_z^e\right) \right], \quad (8)$$

where $E_{\text{tot}}^{He}(M^{He}, S_z^{He})$ is the total energy of the He atom and

$$E^e\left(M^e, S_z^e\right) = \left(M^e + |M^e| + 2S_z^e + 1\right)\frac{B}{2} \quad (9)$$

is the energy of a single electron in a magnetic field. The quantum numbers must satisfy

$$M = M^{He} + M^e, \quad S_z = S_z^{He} + S_z^e. \quad (10)$$

We consider only those states that satisfy conservation of orbital angular momentum and spin, as given in (10), and calculate the threshold energy using (8). Once the threshold is found, the binding energy can be obtained from

$$E_{\text{ion}} = E_{\text{tot}} - E_T. \quad (11)$$

The procedure is analogous for H^{2-}/H^-, Li/Li^+, and Be^+/Be^{2+}. The states with orbital angular momentum and spin considered in the present work are shown in Table I.

C. Physical quantities

The following physical quantities are used to describe the properties of the system and characterize the quality of the wave function: The virial ratio η is defined as

$$\eta = -2\frac{\langle\Psi|T|\Psi\rangle}{\langle\Psi|V|\Psi\rangle} \quad (12)$$

$$= -2\frac{\langle\Psi|T|\Psi\rangle}{\langle\Psi|V_{ee} + V_{Ne}|\Psi\rangle - 2\langle\Psi|V_{ho}|\Psi\rangle}. \quad (13)$$

TABLE I. Spin and angular momentum configurations considered in the present work. ν is the degree of excitation, and π is the parity of the state in the z direction. For all cases, only the lowest degree of excitation with positive parity was considered.

Quantum numbers	Single particle	$\nu^{2S+1}(M)^{\pi}$
$M = 0, S_z = -\frac{1}{2}$	$1s^2 2s$	$^2(0)^+$
$M = -1, S_z = -\frac{1}{2}$	$1s^2 2p_{-1}$	$^2(-1)^+$
$M = -1, S_z = -\frac{3}{2}$	$1s2s2p_{-1}$	$^4(-1)^+$
$M = -3, S_z = -\frac{3}{2}$	$1s2p_{-1}3d_{-2}$	$^4(-3)^+$

Checking how close η is to the ideal value of 1 gives a useful measure of the quality of the wave function [40]. The pair correlation function is defined as

$$C_{ee}(\mathbf{r}) = \frac{2}{N(N-1)}\langle\Psi|\sum_{i<j}^{N}\delta(\mathbf{r}_i - \mathbf{r}_j - \mathbf{r})|\Psi\rangle. \quad (14)$$

Using $C_{ee}(r)$, the radial part of the correlation function, the powers of interparticle distances are given by

$$\langle r_{ee}^k\rangle = 4\pi\int_0^\infty r^k C_{ee}(r) r^2 dr, \quad (15)$$

In a similar manner, the correlation function can also be defined for single particles by taking the distance from the origin instead:

$$C_{Ne}(\mathbf{r}) = \frac{1}{N}\langle\Psi|\sum_{i=1}^{N}\delta(\mathbf{r}_i - \mathbf{r})|\Psi\rangle. \quad (16)$$

Using this correlation function, the square distances between the nucleus and electrons are defined as

$$\rho_{Ne}^2 = 2\pi\int_0^\infty \rho^2 C_{Ne}(\rho)\rho d\rho \quad (17)$$

and

$$z_{Ne}^2 = \int_{-\infty}^{\infty} z^2 C_{Ne}(z) dz. \quad (18)$$

Distances between particles in a bound system are small, and the particles are confined into distances of a few atomic units. Loosely bound systems tend to be larger, up to a few tens of atomic units, but still finite. In unbound systems the distances diverge.

Another quantity of interest is the quadrupole moment, which is defined, as in Ref. [30], as

$$Q_{zz} = \langle\Psi|\sum_{i=1}^{N} 2z_i^2 - \rho_i^2|\Psi\rangle = N(2z_{Ne} - \rho_{Ne}). \quad (19)$$

III. RESULTS AND DISCUSSION

We have calculated the energies of the three-electron isoelectronic series with nuclear charge $Z = 1$–4 for different values of strong magnetic fields for bound states with different angular momentum and spin configurations. $N = 400$ basis functions are used unless otherwise noted.

To test the accuracy of our results we compare our calculation for the energies of low-lying states of the Li atom to Ref. [1], the most accurate results found in the literature. The calculations presented in Ref. [1] are based on Hylleraas-type basis functions and are expected to be very accurate for weak magnetic fields. For higher fields, the Hylleraas description needs many high orbital momentum states and becomes computationally very expensive.

Table II shows the present results and the energies predicted by the Hylleraas approach. For low fields the two calculations are in complete agreement. In the free-field case it is very hard to compete with the accuracy of the Hylleraas approach. One has to use $N = 2000$ basis functions to reach accuracy up to six decimal places. For higher fields the Hylleraas basis seems to be less accurate, and our results improve the previous energies at the third decimal. There is one case, the $^2(-2)^+$ state with $B = 0.009$, where our energy is significantly different from that of Ref. [4]. As other energies in this magnetic field region agree perfectly, we suspect that there might be a typo in Ref. [4].

Using our approach, we have studied the low-lying positive-parity states shown in Table I. These states can be either ground states or lowest excited states depending on the strength of the magnetic field. The evolution of the ground state as a function of the strength of the magnetic field as predicted

TABLE II. The energies (in a.u.) for Li in various configurations calculated in the present work and compared to the values in Ref. [4]. The standard uncertainty is shown in parentheses where applicable. Our calculations are converged up to the six decimal places.

	$^2(0)^+$		$^2(-1)^+$		$^2(-2)^+$	
B	Energy	Ref. [4]	Energy	Ref. [4]	Energy	Ref. [4]
0	−7.478 060 320	−7.478 060 323	−7.410 156 508	−7.410 156 524	−7.335 523 535	−7.335 523 537
0.001	−7.478 558 8	−7.478 558 8(1)	−7.411 153 7	−7.411 153 9(2)	−7.336 509 7	−7.336 500 7(2)
0.0018	−7.478 955 4	−7.478 955 5(2)	−7.411 947 5	−7.411 9475(1)	−7.338 189 4	−7.338 189 4(1)
0.009	−7.482 436 5	−7.482 436 7(2)	−7.418 932 0	−7.418 9321(2)	−7.347 954 1	−7.348 185 6(1)
0.01	−7.482 907 5	−7.482 907 6(1)	−7.419 879 5	−7.419 879 5(1)	−7.349 208 9	−7.348 823 7(1)
0.018	−7.486 566 1	−7.486 566 8(3)	−7.427 265 4	−7.427 2656(2)	−7.349 501 5	−7.358 501 7(1)
0.02	−7.487 450 5	−7.487 451 9(2)	−7.429 059 0	−7.429 059 0(1)	−7.360 614 0	−7.360 448 1(2)
0.2	−7.529 806 2	−7.529 807 (1)	−7.538 656 3	−7.538 654 8(4)	−7.458 826 2	−7.458 823 8(1)
0.4	−7.531 275 5	−7.531 188 7(2)	−7.610 167 0	−7.610 130 7(2)	−7.510 686 6	−7.510 607 6(2)
0.5	−7.523 946 2	−7.523 918 (6)	−7.637 0223 7	−7.636 927 4(3)	−7.528 106 1	−7.528 018 7(1)
0.54	−7.520 090 0	−7.520 016 (1)	−7.646 547 4	−7.646 491 6(1)	−7.533 948 3	−7.533 850 (1)
0.6	−7.513 531 7	−7.513 400 (2)	−7.659 690 7	−7.659 533 (3)	−7.541 677 5	−7.541 506 (3)
0.7	−7.501 000 4	−7.500 958 (7)	−7.678 861 1	−7.678 598 (3)	−7.552 080 7	−7.551 717 (2)
0.9	−7.471 717 4	−7.471 460 (2)	−7.708 359 3	−7.707 760 (1)	−7.564 823 8	
1	−7.455 437 7	−7.454 284 (1)	−7.719 225 9	−7.718 357 (4)	−7.567 629 82	−7.566 400 (1)

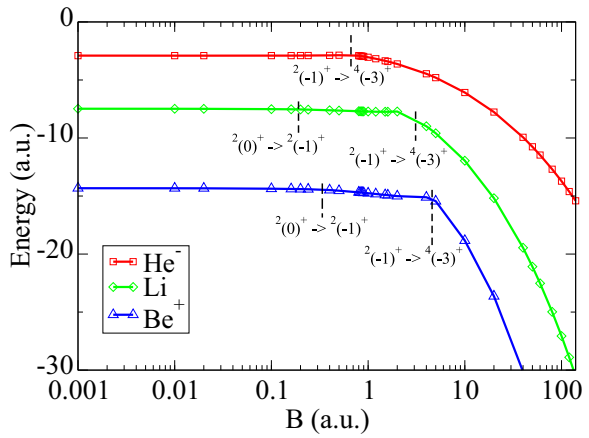

FIG. 1. (Color online) Ground-state energies for different values of magnetic field in He^- (red squares), Li (green diamonds), and Be^+ (blue triangles). The regions where the ground state of the system makes a transition are marked.

by our calculations is shown in Fig. 1. For Li and Be^+ the ground state is the $^2(0)^+$ configuration for low fields, $^2(-1)^+$ for intermediate fields, and $^4(-3)^+$ for very high fields. The ground state of He^- is the $^2(-1)^+$ configuration for smaller values of B [5,40], rather than the $^2(0)^+$ configuration, which is not bound. However, for higher values the ground state of He^- follows the same pattern as that of Li and Be^+.

The ground-state transition points for three-electron systems have been studied in several papers [7,8,30,38]. The calculation of the precise location of the ground-to-excited-state transition points requires very high accuracy for both states, and that is computationally expensive. For the case of Li, the transition has been predicted to be at $B = 2.153$ a.u. [30] and $B = 2.19816$ a.u. [7]. In the case of Be^+, the crossover was estimated to take place at around $B = 4.501$ a.u. in Ref. [36] and $B = 4.55328$ a.u. [7].

Our calculation is in good agreement with these predictions (see Fig. 1). To illustrate the capability of our approach to predict accurate transition points, we have calculated the energies of the $^4(-3)^+$ state for magnetic-field strengths where

TABLE III. Energies at the transition points from $^2(-1)^+$ to the high-magnetic-field ground state $^4(-3)^+$. Here the parameter $\beta_z = \frac{B}{2Z^2}$ is used, just as defined in Ref. [7].

		Energy (a.u.)	
Z	β_z	Present work	Ref. [7]
3	0.12212	−7.69806	−7.6905(3)
4	0.14229	−15.07530	−15.067(6)
5	0.15510	−24.94961	−24.9386(9)
6	0.16404	−37.32606	−37.309(2)
7	0.17059	−52.20168	−52.184(2)
8	0.17556	−69.56932	−69.551(2)
9	0.17947	−89.44020	−89.418(4)
10	0.18266	−111.81031	−111.783(4)

the transition to the $^2(-1)^+$ state takes place, according to Ref. [7], and we have compared the calculations to their predictions for different Z. As Table III shows, the calculated energies using the present method are more negative than those found in Ref. [7], but the general agreement is good.

At the transition points the total energies of the two configurations become equal. However, the structure of the two states can be very different. This is illustrated for He^- in Fig. 2.

In the following, we discuss the bound-state properties of the three-electron systems. We have found bound states for only the He, Li^+, and Be^{++} nuclei. For H^{2-} we have considered the cases shown in Table I and carefully optimized the basis functions to explore possible bound states. No bound state was found, and it seems highly unlikely that a single positive charge can support a bound three-electron state in a magnetic field.

A. The $^2(0)^+$ ($M = 0$, $S_z = -\frac{1}{2}$) configuration

For $Z \leqslant 4$ only the Li atom and the Be^+ ion are bound. The threshold energy is defined by the energy of the Li^+ and Be^{2+} ions with $M = 0$, $S_z = 0$ for all values of the magnetic field. The calculated energies are presented in Table IV for Li and

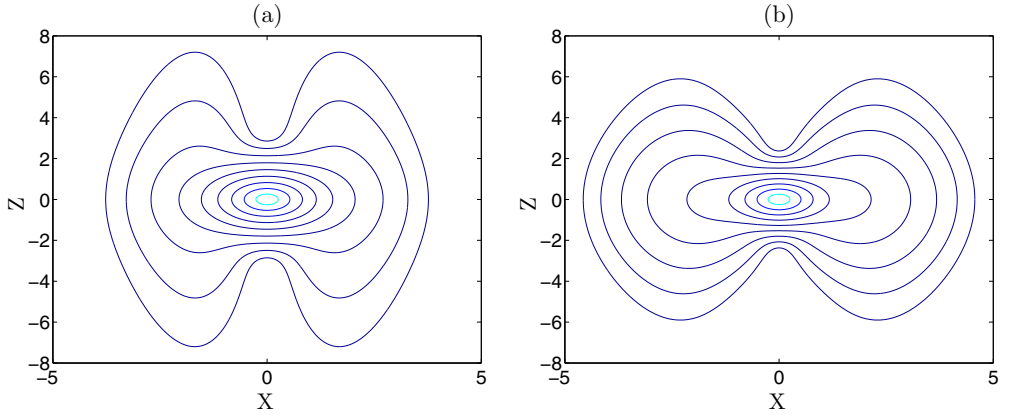

FIG. 2. (Color online) Density contour plots of He^- at the transition point. Neighboring lines differ from each other by factor of e. (a) $M = -1$, $S_z = -\frac{1}{2}$ near the transition point for $B = 0.70416$ a.u. (b) $M = -3$, $S_z = -\frac{3}{2}$ near the transition point for $B = 0.70416$ a.u. x and z are given in a.u.

TABLE IV. The energies (in a.u.) for Li for the present work and some previous ones from other works are shown. When applicable, the standard uncertainty is shown in parenthesis. Our calculations are converged up to the six decimal places.

Li	$^2(0)^+$		$^2(-1)^+$		$^4(-3)^+$		$^4(-1)^+$	
B	Present	Previous	Present	Previous	Present	Previous	Present	Previous
0	−7.478060	−7.478060323 [4]	−7.410157	−7.410 156 524 [4]	−5.142788	−5.142319 [1]	−5.368001	−5.358 88 [30]
		−7.4777957 [67]		−7.4097907 [67]		−5.083 79 [30]		−5.366705 [1]
		−7477766 [1]		−7.407126 [1]				
		−7.4763360 [48]		−7.408803 [48]				
		−7.432 75 [30]		−7.365 09 [30]				
0.001	−7.478559	−7.478 558 8(1) [4]	−7.411154	−7.411 153 9(2) [4]	−5.145754	−5.145464 [1]	−5.369998	−5.360 88 [30]
		−7.478032 [1]		−7.408174 [1]		−5.086 79[30]		−5.368015 [1]
0.0018	−7.478955	−7.478 955 5(2) [4]	−7.411948	−7.411 947 5(1) [4]				
0.009	−7.482437	−7.482 436 7(2) [4]	−7.418932	−7.418 932 1(2) [4]				
0.01	−7.482907	−7.482 907 6(1) [4]	−7.419787	−7.419 879 5(1) [4]	−5.169195	−5.112 68 [30]	−5.387821	−5.378 71 [30]
		−7.482888 [1]		−7.416994 [1]		−5.169111 [1]		−5.385841 [1]
0.018	−7.486566	−7.486 566 8(3) [4]	−7.427265	−7.427 265 6(2) [4]				
0.02	−7.487450	−7.4874519(2) [4]	−7.429059	−7.429 059 0(1) [4]	−5.191562	−5.139 60 [30]	−5.407287	−5.398 17 [30]
		−7.44214 [30]		−7.4856398 [48]				
		−7.490983 [1]						
0.1	−7.514011	−7.5140478(4) [4]	−7.487304	−7.4873396(3) [4]	−5.341001	−5.321 40 [30]	−5.550708	−5.321 40 [30]
		−7.5137817 [67]		−7.4869343 [67]		−5.341030 [1]		−5.550268 [1]
		−7.517154 [1]		−7.484773 [1]				
		−7.5122102 [48]		−7.4858382 [48]				
0.16	−7.525201		−7.519899		−5.453736		−5.645657	
0.2	−7.529806	−7.529807(1) [4]	−7.538656	−7.5386548(4) [4]	−5.525281	−5.511 51 [30]	−5.704017	−5.694 51 [30]
		−7.533495 [1]		−7.536032 [1]		5.524939 [1]		−5.703511 [1]
		−7.5278376 [48]		−7.5366925 [48]				
0.24	−7.532503	−7.532562(2) [4]	−7.555389	−7.5554917(1) [4]	−5.593680		−5.759018	
		−7.5322949 [67]		−7.5549851 [67]				
0.4	−7.531276	−7.531 188 7(2) [4]	−7.610167	−7.610 130 7(2) [4]	−5.842165		−5.953098	
0.5	−7.523946	−7.523918(6) [4]	−7.637022	−7.6369274(3) [4]	−5.982239	−5.970 52 [30]	−6.058881	−6.047 87 [30]
		−7.5235946 [67]		−7.6362483 [67]		−5.982253 [1]		−6.058463 [1]
		−7.528055 [1]		−7.634547 [1]				
		−7.5216127 [48]		−7.6341245 [48]				
		−7.477 41 [30]		−7.587 90 [30]				
0.54	−7.520090	−7.520 016 (1) [4]	−7.646547	−7.646 491 6(1) [4]				
0.6	−7.513532	−7.513 400 (2) [4]	−7.659691	−7.659 533 (3) [4]				
0.7	−7.501000	−7.500 958 (7) [4]	−7.678861	−7.678 598 (3) [4]				
0.8	−7.486909		−7.694877		−6.358064		−6.333199	
0.9	−7.471717	−7.425 04 [30]	−7.708359	−7.707760(1) [4]	−6.472200	−6.460 61 [30]	−6.415307	−6.401 75 [30]
		−7.471460(2) [4]		−7.707054 [67]				
		−7.4710527 [67]						
1	−7.455438	−7.458550 [1]	−7.719226	−7.718357(4) [4]	−6.582402	−6.570 81 [30]	−6.494473	−6.480 29 [30]
		−7.454284(1) [4]		−7.716679 [1]		−6.582361 [1]		−6.494196 [1]
		−7.4529046 [48]		−7.7151944 [48]				
		−7.408 79 [30]		−7.66653 [30]				
1.2	−7.419998		−7.734021		−6.792757		−6.646298	
1.5	−7.360140		−7.741348		−7.086491		−6.863210	
1.6	−7.338404		−7.740137		−7.179497		−6.933452	
2	−7.242189	−7.19621 [30]	−7.719430	−7.662 46 [30]	−7.532720	−7.520 03 [30]	−7.206104	−7.188 89 [30]
		−7.244919 [1]		−7.715709 [1]		−7.530125 [1]		−7.206026 [1]
4	−6.566910		−7.328330		−8.989213		−8.397667	
5	−6.133931	−6.08811 [30]	−7.005519	−7.002346 [1]	−9.592108	−9.591769 [1]	−8.905753	−8.905985 [1]
		−6.136918 [1]		−6.942 30 [30]		−9.576 94 [30]		−8.889 81 [30]
10	−3.404618	−3.35777 [30]	−4.687628	−4.617 77 [30]	−11.957598	−11.939 02 [30]	−10.925795	−10.910 59 [30]
		−3.406556 [1]		−4.684076 [1]		−11.957294 [1]		−10.925976 [1]
20	3.441799	3.49120 [30]	1.625407	1.705 65 [30]	−15.186392	−15.162 60 [30]	−13.709466	−13.694 20 [30]
40	19.241172		16.740670		−19.457466		−17.405439	
50	27.634711	27.6916 [30]	24.875829	24.979 42 [30]	−21.086742	−21.0505[30]	−18.818393	−18.8012 [30]
60	36.221250		33.236274		−22.519774		−20.061769	
80	53.795996		50.424092		−24.979924		−22.196659	
100	71.741025	71.807 [30]	68.041685	68.1735 [30]	−27.065453	−27.0192 [30]	−24.006455	−23.987 [30]

TABLE V. The energies (in a.u.) for Be^+. Our calculations are converged up to the five decimal places.

Be^+	$M=0, S_z=-\frac{1}{2}$		$M=-1, S_z=-\frac{1}{2}$		$M=-3, S_z=-\frac{3}{2}$		$M=-1, S_z=-\frac{3}{2}$	
B	Present	Previous	Present	Previous	Present	Previous	Present	Previous
0	−14.32472	−14.3247 [35]	−14.17927	−14.17608 [41]	−9.43565	−9.4156 [35]	−10.06663	−10.0650 [35]
0.001	−14.32523	−14.3251[35]	−14.18026	−14.1751 [35]	−9.43864	−9.4185 [35]	−10.06863	−10.0655 [35]
0.01	−14.32966	−14.3296 [35]	−14.18920	−14.1841[35]	−9.46508	−9.4452 [35]	−10.08656	−10.0827 [35]
0.02	−14.33450		−14.19898		−9.49354		−10.10633	
0.1	−14.36936	−14.3694 [35]	−14.27232	−14.2672 [35]	−9.70137	−9.6888 [35]	−10.25911	−10.2575 [35]
0.16	−14.39120		−14.32195		−9.84398		−10.36754	
0.2	−14.40387	−14.4038 [35]	−14.35276	−14.34926 [41]	−9.93417	−9.9243 [35]	−10.43703	−10.4353 [35]
0.24	−14.41515		−14.38196		−10.02097		−10.50440	
0.4	−14.44815	−14.44641 [41]	−14.48546		−10.34197		−10.75466	
0.5	−14.46058	−14.4606 [35]	−14.54155	−14.5358 [35]	−10.52597	−10.5188 [35]	−10.89747	−10.8918 [35]
0.8	−14.47164		−14.68180		−11.02510		−11.27766	
0.825	−14.47118		−14.69178		−11.06384		−11.30667	
0.85	−14.47052		−14.70195		−11.10223		−11.33533	
0.875	−14.46971		−14.71174		−11.14031		−11.36366	
0.9	−14.46873		−14.72135		−11.17799		−11.39166	
1	−14.46333	−14.4630 [35]	−14.75795	−14.75295 [41]	−11.32565	−11.3203 [35]	−11.50059	−11.4967 [35]
1.2	−14.44657		−14.82352		−11.60733		−11.70565	
1.5	−14.41037		−14.90558		−12.00218		−11.98811	
1.6	−14.39610		−14.92917		−12.12764		−12.07702	
2	−14.33123	−14.3300 [35]	−15.00694	−15.0000 [35]	−12.60455	−12.6002 [35]	−12.41340	−12.4090 [35]
4	−13.88655	−13.88455 [41]	−15.10915		−14.59956		−13.86701	
5	−13.59866	−13.5971 [35]	−15.02875	−15.0184 [35]	−15.44204	−15.4367 [35]	−14.51655	−14.5106 [35]
10	−11.62510	−11.6231 [35]	−13.82293	−13.80892 [41]	−18.83615	−18.8283 [35]	−17.24524	−17.2291 [35]
20	−6.08322	−6.08121[41]	−9.28941	−9.27043 [41]	−23.63118		−21.20083	
40	7.76380		3.23746		−30.13352		−26.60687	
50	15.37269	15.4261 [36]	10.34234	10.42836 [36]	−32.64727	−32.61959 [36]	−28.70079	
60	23.25698		17.78248		−34.86928		−30.55231	
80	39.60523		33.36648		−38.70313		−33.74752	
100	56.49203	56.5516 [36]	49.60389	49.7082 [36]	−41.97236	−41.93414 [36]	−36.47142	

in Table V for Be^+. The behavior of the energy as a function of the magnetic field is shown in Fig. 3. The total energy of Li in this configuration has a local minimum, as previously reported in Ref. [30] at $B = 0.304$ a.u. A similar minimum for Be^+ is around $B = 0.8$ a.u., and the general behavior of the two curves is rather similar. The binding energies of these states are shown in Fig. 3. The binding energies first start to increase with the magnetic field, but at a certain maximum point this trend changes, leading to a local minima after which the binding increases again. The minimum values for binding energy are located around $B = 2$ a.u. for Li and $B = 4$ a.u. for Be^+. The shape of the binding energy curve is determined by the difference between the total energy of the three-electron and the total energy of the two-electron system; therefore these curves have a more complicated structure than the three-electron energy curve (see Fig. 3). The maximum values of binding energies were found around $B = 0.4$ a.u. for Li and $B = 1.2$ a.u. for Be^+. It is important to point out that the systems undergo significant structural changes near those regions. In the interval 0.24 a.u. $< B <$ 0.4 a.u. Li becomes more elongated along the z direction and then changes back to being a less prolate shape, as seen in Fig. 3 (see also the quadrupole moments for Li and Be^+ in Table VI). For the case of Be^+ a similar expansion is observed in Fig. 3 for Z_{Ne}^2 but around the interval 0.8 a.u. $< B <$ 4 a.u.

The energies become positive as B increases because $\langle V_{\rm mag}\rangle$ becomes positive, and the kinetic energy gets substantially larger, as illustrated in Tables VII and VIII. This is due to the increase of the harmonic oscillator contribution $\langle V_{ho}\rangle$. For small fields the largest contribution to the total energy comes from the electron-nuclear attraction. The kinetic energy $\langle T\rangle$, however, eventually becomes greater in magnitude than $\langle V_{Ne}\rangle$, becoming the dominant term of the Hamiltonian for larger fields.

B. The $^2(-1)^+$ ($M = -1, S_z = -\frac{1}{2}$) configuration

The total energies for He^-, Li, and Be^+ are plotted in Fig. 4 and presented in Tables IV, V, and IX. The corresponding binding energies (see Fig. 4) are calculated by using the threshold energy belonging to the $^1(0)^+$ state of the He atom and Li^+ and Be^{2+} ions for all magnetic fields. The $^2(-1)^+$ state was found to be bound for Li and Be^+ for all values of B, but the He^- ion is bound only for certain B field intensities.

The $^2(-1)^+$ configuration has a local minimum in total energy for Li and Be^+ (Fig. 4). However, there is no minimum observed for He^-; its total energy is monotonously increasing. This shows that the minimum in the energy curves of Li and Be^+ is due to the competition between the attractive nuclear Coulomb potential and the magnetic interaction. In the Li atom and the Be^+ ion the magnetic field forces the electron closer

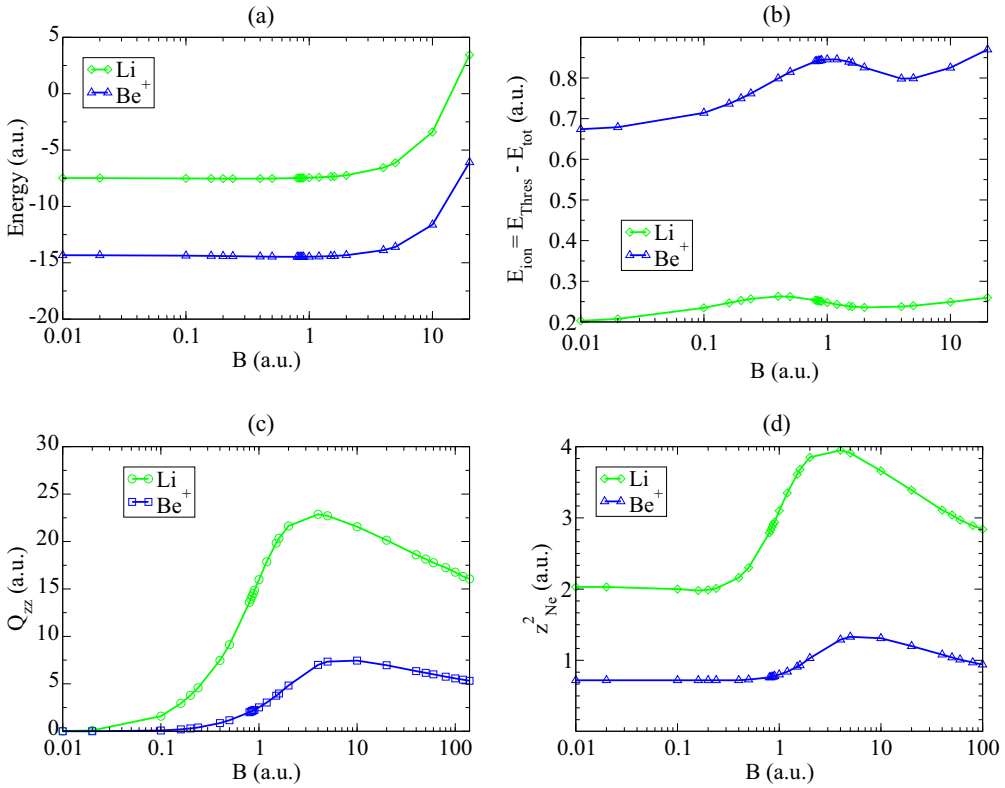

FIG. 3. (Color online) State with $^2(0)^+$ ($M = 0$, $S_z = -\frac{1}{2}$). (a) Total energies, (b) binding energies, (c) Q_{zz}, and (d) average z_{Ne}^2 for Li and Be^+.

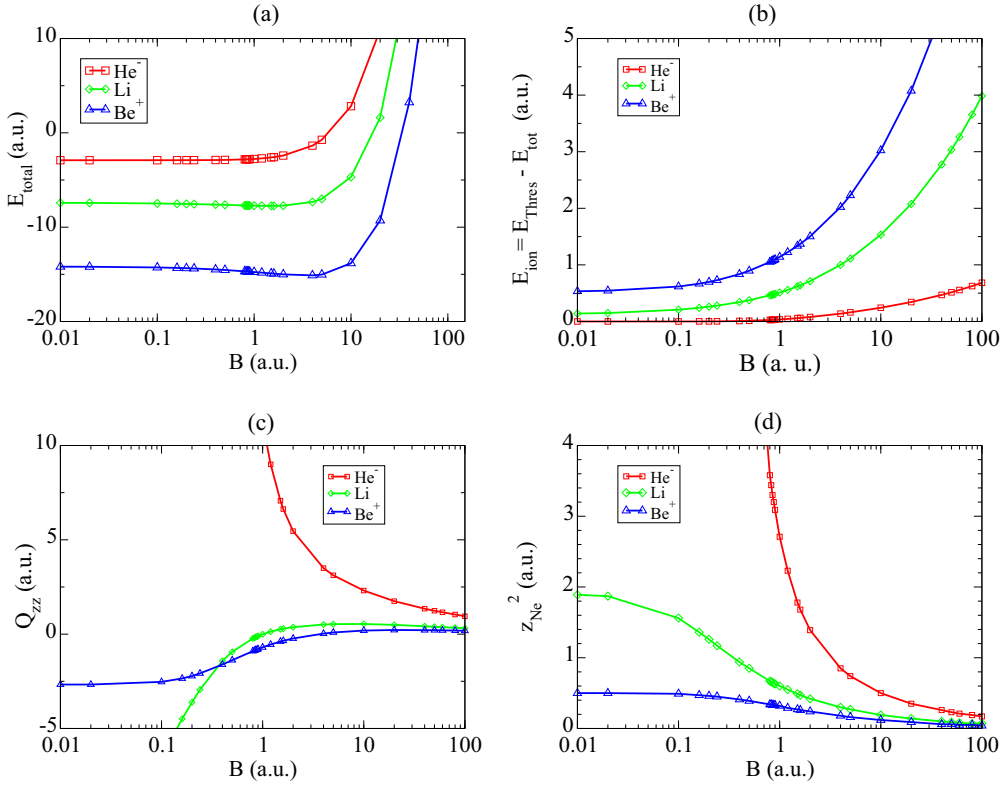

FIG. 4. (Color online) State with $^2(-1)^+$ ($M = -1$, $S_z = -\frac{1}{2}$). (a) Total energies, (b) binding energy, (c) Q_{zz}, and (d) average z_{Ne}^2.

TABLE VI. Quadrupole moments Q_{zz} for the different systems and configurations.

B	He^-			Li				Be^+			
	$^2(-1)^+$	$^4(-3)^+$	$^4(-1)^+$	$^2(0)^+$	$^2(-1)^+$	$^4(-3)^+$	$^4(-1)^+$	$^2(0)^+$	$^2(-1)^+$	$^4(-3)^+$	$^4(-1)^+$
0			−48.16	0.00	−10.81	−217.96	−4.49	0.00	−2.67	−31.03	−1.72
0.001			−48.70	0.00	−10.79	−217.10	−4.49	0.00	−2.67	−31.05	−1.72
0.01			−36.38	0.02	−10.70	−170.37	−4.48	0.00	−2.67	−30.18	−1.72
0.02		108.31	−26.66	0.09	−10.41	−124.50	−4.45	0.00	−2.67	−28.00	−1.72
0.1	1,038.67	−22.19	−0.50	1.59	−6.49	−25.48	−3.73	0.08	−2.53	−13.69	−1.66
0.16	411.16	−9.76	8.82	2.94	−4.49	−15.59	−2.92	0.20	−2.35	−10.59	−1.57
0.2	248.97	−5.68	14.41	3.79	−3.61	−12.68	−2.36	0.30	−2.22	−9.32	−1.49
0.24	164.92	−3.09	20.38	4.58	−2.94	−10.74	−1.82	0.40	−2.08	−8.34	−1.41
0.4	53.34	1.70	65.25	7.47	−1.42	−6.47	0.10	0.86	−1.61	−5.89	−1.02
0.5	34.76	2.87	161.95	9.11	−0.94	−5.04	1.14	1.16	−1.38	−4.96	−0.77
0.8	15.41	4.06		13.59	−0.23	−2.72	3.91	2.00	−0.90	−3.29	−0.03
0.825	14.68	4.09		13.91	−0.19	−2.60	4.13	2.06	−0.87	−3.19	0.02
0.85	14.01	4.16		14.24	−0.16	−2.49	4.35	2.13	−0.84	−3.10	0.08
0.875	13.53	4.19		14.53	−0.13	−2.38	4.57	2.20	−0.82	−3.01	0.14
0.9	13.01	4.20		14.86	−0.10	−2.28	4.79	2.26	−0.79	−2.93	0.19
1	11.21	4.27		15.98	−0.01	−1.91	5.65	2.52	−0.70	−2.63	0.41
1.2	9.00	4.29		17.87	0.13	−1.37	7.34	3.03	−0.55	−2.16	0.83
1.5	7.07	4.26		19.84	0.26	−0.83	9.68	3.75	−0.39	−1.66	1.42
1.6	6.63	4.19		20.34	0.29	−0.70	10.39	3.98	−0.35	−1.53	1.61
2	5.46	4.07		21.63	0.37	−0.31	12.78	4.82	−0.23	−1.13	2.34
4	3.50	3.44		22.87	0.51	0.38	17.65	7.00	0.03	−0.30	4.99
5	3.12	3.21		22.71	0.53	0.49	18.33	7.34	0.09	−0.14	5.64
10	2.31	2.59		21.56	0.54	0.63	19.04	7.45	0.19	0.16	6.52
20	1.75	2.05		20.14	0.49	0.61	18.60	6.96	0.22	0.26	6.43
40	1.35	1.58		18.61	0.42	0.53	17.72	6.34	0.21	0.27	6.04
50	1.24	1.47		18.15	0.39	0.50	17.39	6.16	0.21	0.26	5.89
60	1.16	1.36		17.77	0.37	0.47	17.15	6.00	0.20	0.25	5.77
80	1.04	1.23		17.24	0.34	0.43	16.70	5.75	0.19	0.24	5.58
100	0.95	1.12		16.77	0.31	0.39	16.44	5.57	0.18	0.23	5.43
120	0.88	1.05		16.32	0.30	0.37	16.09	5.44	0.17	0.21	5.31
140	0.81	0.98		16.06	0.28	0.35	15.94	5.32	0.16	0.20	5.20
200		0.80			0.14		15.65	5.05	0.14		4.98
300		0.70			0.12		15.12	4.84	0.12		4.73
400		0.62			0.11		15.11		0.11		4.61
500		0.56			0.10		14.90		0.10		4.54
600		0.52			0.10		15.05		0.10		4.49
700		0.42			0.09		18.05		0.09		4.47
800		0.47			0.09		17.60		0.09		4.30
900					0.08				0.08		4.37

to the nucleus, and that decreases the energy up to a certain B value. In the He^- ion the $Z = 2$ charge is not strong enough to produce the same effect.

The He^- ion in this configuration is not bound without a magnetic field, and according to the present calculation, a minimal field strength $B = 0.062(6)$ a.u. is needed for a bound He^- ion. This is a slight improvement over previous works [5,40]. Determining a more accurate value is possible but computationally expensive.

The boundedness of the He^- ion can be explained by the magnetic ($\langle V_{\rm mag}\rangle$) contribution to the energy, which is plotted for He^- and Li as a function of B in Fig. 5. This figure also shows the curves for He and Li^+ in $1^1(0)^+$, which define the threshold energies. As Fig. 5 shows, the contribution of the magnetic field $\langle V_{\rm mag}\rangle$ is negative for the three-electron case, and this supports bound systems. The system is naturally bound for all values of magnetic field for Li (and Be^+) where the nuclear Coulomb contribution is enough to bind the electron even without a magnetic field. For He^-, this additional $\langle V_{\rm mag}\rangle$ becomes strong enough to make the system bound for larger B values.

The quadrupole moments of the systems in the $^2(-1)^+$ configuration are compared in Fig. 4 and in Table VI. The weakly bound He^- ion has a prolate shape and becomes gradually more spherical as the magnetic field increases. Li and Be^+ have oblate shapes at low magnetic fields and change to prolate shapes after the magnetic field becomes strong enough.

C. The $^4(-1)^+$ ($M = -1$, $S_z = -\frac{3}{2}$) configuration

The total energies for this case are presented in Tables IV, V, and IX and plotted in Fig. 6. Both Li and Be^+ are stable in this

TABLE VII. Energy contribution (in a.u.) of different terms of the Hamiltonian for the $^2(0)^+$ ($M = 0$, $S_z = -\frac{1}{2}$) configuration of Li.

B	$\langle T\rangle$	$\langle V_{ee}\rangle$	$\langle V_{Ne}\rangle$	$\langle V_{ho}/B\rangle$	$\langle V_{\rm mag}/B\rangle$	$E_{\rm tot}$
0	7.478	2.198	−17.154			−7.478
0.001	7.478	2.198	−17.154	0.002	−0.498	−7.479
0.01	7.478	2.199	−17.155	0.015	−0.485	−7.483
0.02	7.479	2.200	−17.156	0.030	−0.470	−7.487
0.1	7.503	2.225	−17.205	0.130	−0.370	−7.514
0.16	7.531	2.251	−17.257	0.180	−0.320	−7.525
0.2	7.552	2.268	−17.291	0.205	−0.295	−7.530
0.24	7.574	2.284	−17.325	0.225	−0.275	−7.533
0.4	7.663	2.334	−17.439	0.277	−0.223	−7.531
0.5	7.716	2.354	−17.492	0.295	−0.205	−7.524
0.8	7.863	2.378	−17.586	0.324	−0.176	−7.487
0.825	7.874	2.379	−17.591	0.325	−0.175	−7.483
0.85	7.885	2.379	−17.596	0.327	−0.173	−7.479
0.875	7.897	2.379	−17.601	0.328	−0.172	−7.476
0.9	7.909	2.380	−17.606	0.329	−0.171	−7.472
1	7.956	2.379	−17.624	0.334	−0.166	−7.455
1.2	8.053	2.379	−17.663	0.343	−0.157	−7.420
1.5	8.213	2.382	−17.739	0.356	−0.144	−7.360
1.6	8.270	2.384	−17.770	0.361	−0.139	−7.338
2	8.516	2.400	−17.917	0.379	−0.121	−7.242
4	10.001	2.543	−18.923	0.453	−0.047	−6.567
5	10.819	2.621	−19.469	0.479	−0.021	−6.134
10	15.088	2.971	−22.025	0.556	0.056	−3.405
20	23.664	3.491	−26.082	0.618	0.118	3.442
40	40.398	4.203	−31.907	0.664	0.164	19.241
50	48.615	4.477	−34.208	0.675	0.175	27.635
60	56.763	4.719	−36.258	0.683	0.183	36.221
80	72.910	5.134	−39.817	0.695	0.195	53.796
100	88.909	5.486	−42.872	0.702	0.202	71.741

TABLE VIII. Energy contribution (in a.u.) of different terms of the Hamiltonian for the $^2(0)^+$ ($M = 0$, $S_z = -\frac{1}{2}$) configuration of Be^+.

B	$\langle T\rangle$	$\langle V_{ee}\rangle$	$\langle V_{Ne}\rangle$	$\langle V_{ho}/B\rangle$	$\langle V_{\rm mag}/B\rangle$	$E_{\rm tot}$
0	14.325	3.246	−31.895			−14.325
0.001	14.324	3.246	−31.894	0.001	−0.499	−14.325
0.01	14.324	3.246	−31.895	0.005	−0.495	−14.330
0.02	14.324	3.246	−31.895	0.011	−0.489	−14.334
0.1	14.335	3.252	−31.911	0.053	−0.447	−14.369
0.16	14.350	3.260	−31.934	0.082	−0.418	−14.391
0.2	14.363	3.267	−31.954	0.101	−0.399	−14.404
0.24	14.379	3.275	−31.977	0.117	−0.383	−14.415
0.4	14.455	3.311	−32.084	0.173	−0.327	−14.448
0.5	14.511	3.335	−32.157	0.201	−0.299	−14.461
0.8	14.690	3.399	−32.367	0.258	−0.242	−14.472
0.825	14.702	3.403	−32.379	0.261	−0.239	−14.471
0.85	14.717	3.408	−32.394	0.265	−0.235	−14.471
0.875	14.733	3.412	−32.411	0.268	−0.232	−14.470
0.9	14.748	3.417	−32.427	0.271	−0.229	−14.469
1	14.807	3.433	−32.485	0.283	−0.217	−14.463
1.2	14.925	3.460	−32.591	0.301	−0.199	−14.447
1.5	15.092	3.488	−32.718	0.319	−0.181	−14.410
1.6	15.146	3.495	−32.754	0.324	−0.176	−14.396
2	15.354	3.512	−32.871	0.338	−0.162	−14.331
4	16.485	3.561	−33.465	0.383	−0.117	−13.887
5	17.163	3.607	−33.890	0.404	−0.096	−13.599
10	21.116	3.901	−36.472	0.483	−0.017	−11.625
20	29.700	4.435	−41.425	0.560	0.060	−6.083
40	46.872	5.217	−49.204	0.622	0.122	7.764
50	55.330	5.526	−52.386	0.638	0.138	15.373
60	63.717	5.799	−55.251	0.650	0.150	23.257
80	80.309	6.271	−60.281	0.666	0.166	39.605
100	96.722	6.674	−64.642	0.677	0.177	56.492

configuration for all tested B fields. The He^- ion is stable in the $B = [0,0.63]$ a.u. region, but it becomes unbound beyond that value [40,45].

The threshold energies are the energies of the He atom and the Li^+ and Be^{++} ions in state $^2(0)^+$ or $^2(-1)^+$, depending on the intensity of the B field. In the case of the He atom, the $^2(0)^+$ configuration has more negative energy for $B \leqslant 0.02$ a.u. At some point within the interval (0.02,0.10] the energy of $^2(-1)^+$ becomes more negative than that of $^2(0)^+$. Therefore it becomes the threshold for larger B fields. For Li^+ the situation is similar, but the interval is (0.16,0.20], while for Be^{++} it is (0.24,0.40]. From the calculation it can be seen that a higher nuclear charge implies that the threshold changes at a higher B field. Note that, unlike in the previous cases, the $1^1(0)^+$ configuration is not a threshold because conservation of angular momentum forbids the transition to that state within the nonrelativistic framework [see Eq. (10)].

The binding energy for He^-, Li, and Be^+ is shown in Fig. 6. For all three systems a maximum and a minimum can be observed. In the case of Li and Be^+ the binding energy keeps increasing at high fields. Further details can be seen by comparison of the electron-nucleus distance z^2_{Ne}. The maximum binding energy seems to take place near the point where the elongation in z starts increasing, as shown in Fig. 6. This is similar to the cases described in the previous section.

For Li and Be^+ the minimum binding energy happens to be near the point where z^2_{Ne} is maximum and the systems become less tightly bound. At the same time, the He^- ion becomes unbound as this region is approached.

For low fields He^-, Li, and Be^+ have oblate shapes, although the magnitude of the quadrupole moment of Li and

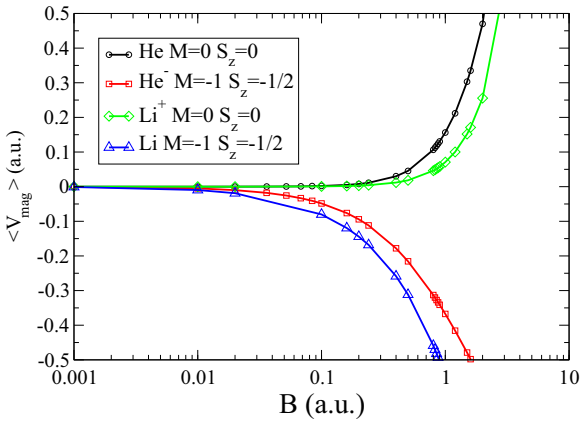

FIG. 5. (Color online) Matrix elements for the magnetic contribution in He^- and Li in the $^2(-1)^+$ state.

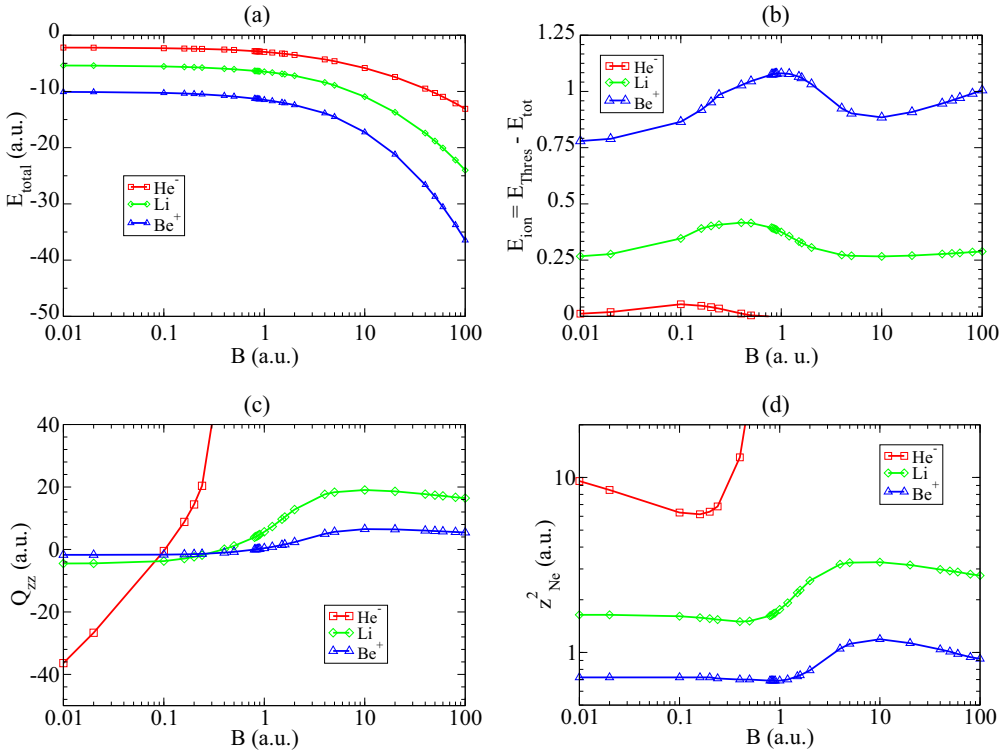

FIG. 6. (Color online) State with $^4(-1)^+$ ($M = -1$, $S_z = -\frac{3}{2}$) for different nuclear charges Z. (a) Total energies, (b) binding energies, (c) Q_{zz}, and (d) average distance z^2_{Ne} for different values of magnetic field.

Be^+ is much smaller than that of He^-. By increasing the magnetic field the shape of these systems becomes prolate, forming needlelike structures in high magnetic field.

D. The $^4(-3)^+$ ($M = -3$, $S_z = -\frac{3}{2}$) configuration

The energies for this configuration are shown in Fig. 7 and presented in Tables IV, V, and IX. This state is fully spin

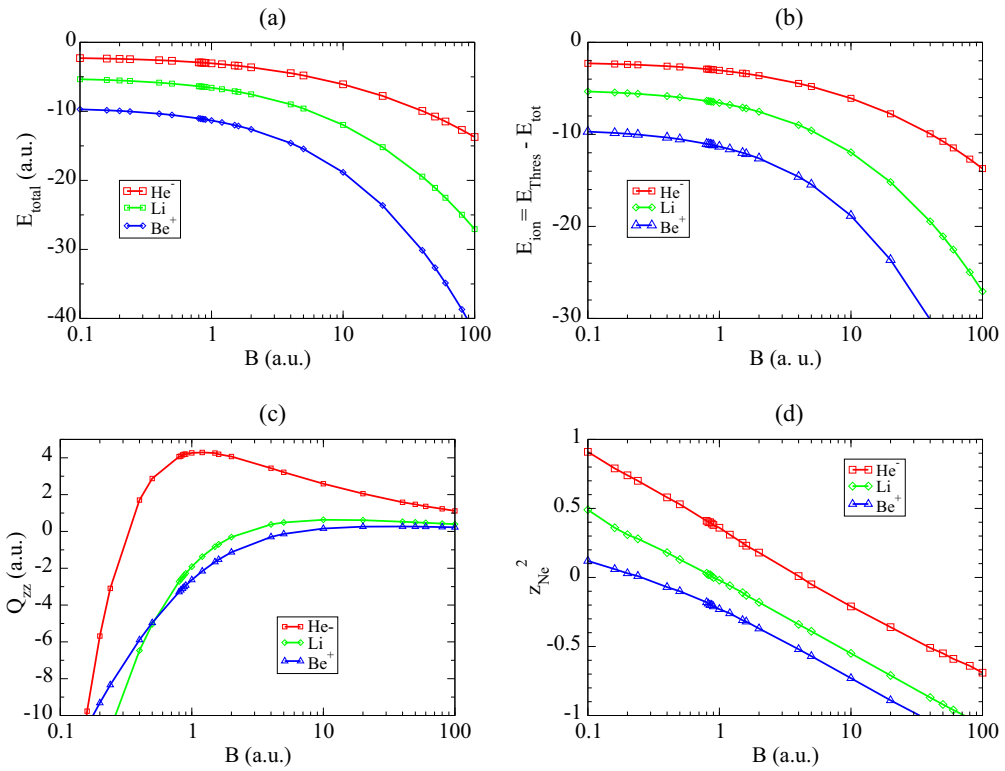

FIG. 7. (Color online) State with $^4(-3)^+$ ($M = -3$, $S_z = -\frac{3}{2}$). (a) Total energies, (b) binding energy, (c) Q_{zz}, and (d) average z^2_{Ne}.

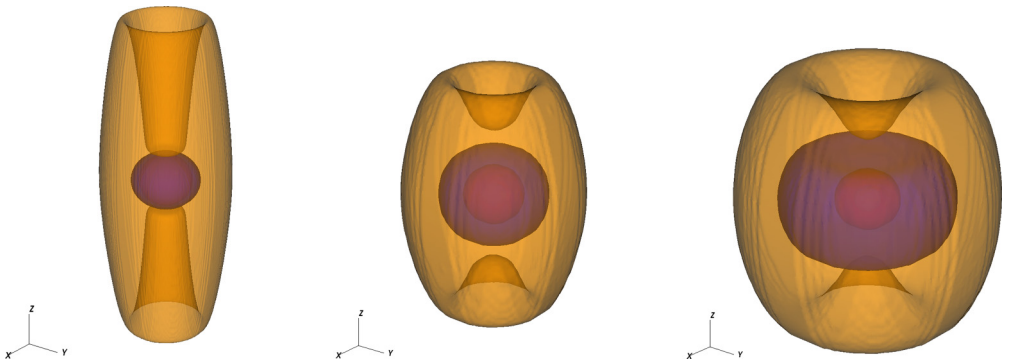

FIG. 8. (Color online) Density 3D contour plots for He^-: (a) $^2(-1)^+$ with $B = 0.1$ and (b) state $^2(-1)^+$ and (c) state $^4(-3)^+$, both with $B = 0.70416$, which is near the transition point.

polarized and eventually becomes the ground state at higher B fields for He^-, Li, and Be^+, as shown in Fig. 1.

The threshold for this state is similar to that of the $^4(-1)^+$ configuration, corresponding to configurations $^2(0)^+$ and $^2(-1)^+$ of the two-electron systems, as explained before. He^- $^4(-3)^+$ is not stable below $B = 0.02$ a.u., but for stronger fields it does becomes stable, and it is the ground state at higher fields.

TABLE IX. The energies (in a.u.) for the bound states of He^-. Our calculations are converged up to the five decimal places.

B	$^2(-1)^+$	$^4(-3)^+$	$^4(-1)^+$
0			−2.17799
0.001			−2.17999
0.01			−2.19675
0.02		−2.19486	−2.21359
0.1	−2.90195	−2.28616	−2.31516
0.16	−2.89955	−2.35633	−2.37213
0.2	−2.89745	−2.39957	−2.40571
0.24	−2.89495	−2.44063	−2.43711
0.4	−2.88081	−2.58980	−2.55322
0.5	−2.86844	−2.67456	−2.62430
0.8	−2.81491	−2.90426	
0.825	−2.80935	−2.92208	
0.85	−2.80366	−2.93975	
0.875	−2.79785	−2.95722	
0.9	−2.79187	−2.97460	
1	−2.76647	−3.04235	
1.2	−2.70918	−3.17123	
1.5	−2.60862	−3.35047	
1.6	−2.57169	−3.40693	
2	−2.40919	−3.61936	
4	−1.35729	−4.46404	
5	−0.73685	−4.80152	
10	2.82088	−6.08238	
20	10.92288	−7.76693	
40	28.47898	−9.93814	
50	37.55970	−10.75595	
60	46.75611	−11.47044	
80	65.38648	−12.69037	
100	84.23329	−13.71707	

Tables X and XI show the energy contributions for Li and He^-. Note that $\langle V_{Ne}\rangle$ is always more negative for the $^2(-1)^+$ configuration than for the $^4(-3)^+$ case (see Tables VII and XI). On the other hand, $\langle V_{\rm mag}\rangle$ is always more negative for the $^4(-3)^+$ case since it is fully spin polarized. The electron repulsion tends to be less significant for $^4(-3)^+$ than $^2(-1)^+$ for all three-electron systems. This shows that having a higher angular momentum allows a reduction of the electron repulsion while simultaneously decreasing the Coulombic attraction due to the larger distances. For large magnetic fields, having larger angular momenta is energetically favored since it allows for the alignment of the magnetic moments with the external field, giving a more negative $\langle V_{\rm mag}\rangle$. This eventually leads to crossover, and the $^4(-3)^+$ state becomes the ground state. Comparing Tables X and XI, one sees that due to the difference in nuclear charge the contribution of $\langle V_{Ne}\rangle$ is much larger for Li than for He^-, which also induces larger kinetic energy for Li. At the same time the magnetic contribution is comparable in the two systems, and the strong magnetic contribution supports the bound state of the He^- ion.

TABLE X. Energy contribution (in a.u.) of different terms of the Hamiltonian for the $^4(-3)^+$ ($M = -3$, $S_z = -\frac{3}{2}$) configuration of He^-.

B	$\langle T\rangle$	$\langle V_{ee}\rangle$	$\langle V_{Ne}\rangle$	$\langle V_{ho}/B\rangle$	$\langle V_{\rm mag}/B\rangle$	$E_{\rm tot}$
0.160	2.329	0.587	−4.943	0.943	−2.057	−2.356
0.200	2.384	0.632	−5.011	0.974	−2.026	−2.400
0.240	2.439	0.674	−5.074	0.999	−2.001	−2.441
0.400	2.664	0.811	−5.290	1.062	−1.938	−2.590
0.500	2.807	0.881	−5.406	1.088	−1.912	−2.675
0.800	3.244	1.051	−5.712	1.142	−1.858	−2.904
0.825	3.281	1.063	−5.736	1.145	−1.855	−2.922
0.850	3.318	1.075	−5.759	1.148	−1.852	−2.940
0.875	3.355	1.086	−5.782	1.152	−1.848	−2.957
0.900	3.393	1.098	−5.805	1.155	−1.845	−2.975
1.000	3.543	1.143	−5.895	1.167	−1.833	−3.042
1.200	3.848	1.224	−6.068	1.188	−1.812	−3.171
1.500	4.312	1.331	−6.314	1.214	−1.786	−3.350
1.600	4.468	1.364	−6.393	1.221	−1.779	−3.407
2.000	5.100	1.484	−6.697	1.247	−1.753	−3.619

TABLE XI. Energy contribution (in a.u.) of different terms of the Hamiltonian for the $^4(-3)^+$ ($M = -3$, $S_z = -\frac{3}{2}$) configuration of Li.

B	$\langle T \rangle$	$\langle V_{ee} \rangle$	$\langle V_{Ne} \rangle$	$\langle V_{ho}/B \rangle$	$\langle V_{\rm mag}/B \rangle$	$E_{\rm tot}$
0	5.143	0.595	−10.880	0.000	0.000	−5.143
0.001	5.143	0.594	−10.880	0.036	−2.964	−5.146
0.01	5.148	0.605	−10.896	0.293	−2.707	−5.169
0.02	5.158	0.624	−10.922	0.449	−2.551	−5.192
0.1	5.205	0.800	−11.101	0.550	−2.450	−5.341
0.16	5.254	0.884	−11.205	0.585	−2.415	−5.454
0.2	5.300	0.923	−11.273	0.626	−2.374	−5.525
0.24	5.351	0.957	−11.341	0.664	−2.336	−5.594
0.4	5.571	1.077	−11.600	0.775	−2.225	−5.842
0.5	5.715	1.143	−11.751	0.822	−2.178	−5.982
0.8	6.157	1.313	−12.161	0.917	−2.083	−6.358
0.825	6.194	1.325	−12.192	0.922	−2.078	−6.387
0.85	6.232	1.338	−12.224	0.928	−2.072	−6.416
0.875	6.269	1.350	−12.255	0.934	−2.066	−6.444
0.9	6.306	1.362	−12.286	0.939	−2.061	−6.472
1	6.456	1.409	−12.406	0.958	−2.042	−6.582
1.2	6.758	1.497	−12.635	0.991	−2.009	−6.793
1.5	7.214	1.614	−12.957	1.029	−1.971	−7.086
1.6	7.368	1.650	−13.060	1.039	−1.961	−7.179
2	7.987	1.782	−13.453	1.076	−1.924	−7.533
4	11.172	2.282	−15.172	1.182	−1.818	−8.989
5	12.795	2.477	−15.932	1.214	−1.786	−9.592
10	20.961	3.218	−19.138	1.300	−1.700	−11.958
20	37.143	4.216	−23.864	1.366	−1.634	−15.186
40	68.938	5.547	−30.438	1.412	−1.588	−19.457
50	84.667	6.060	−33.011	1.424	−1.576	−21.087
60	100.328	6.516	−35.299	1.432	−1.568	−22.520
80	131.487	7.302	−39.266	1.444	−1.556	−24.980
100	162.489	7.972	−42.661	1.451	−1.549	−27.065

Figure 7 shows the quadrupole moment and z^2 for this configuration. The behavior of the quadrupole moment for Li and Be^+ is similar to the results shown in Ref. [30]. The system has an oblate shape at small magnetic fields and gradually becomes more spherical for high fields. The change in shape is more noticeable for He^-, which is also oblate for low fields but becomes prolate at around $B = 0.5$ a.u and then changes back to spherical for high fields.

IV. SUMMARY

The energies and the structures of three-electron systems (He^-, Li, and Be^+) have been calculated using deformed explicitly correlated Gaussian basis representation. The basis functions had different parameters in the z direction and the xy plane following the symmetry of the magnetic Hamiltonian. This flexibility allows higher accuracy than other methods using spherical basis states. The basis parameters were optimized by the stochastic variational method, which provides an efficient and simple way to reach highly accurate ground-state energies. The stability of the system as a function of the nuclear charge and magnetic field was analyzed, pointing out the similarities and the differences in the properties of these systems. The approach presented in this paper can be extended to larger systems and work on four- and five-electron systems is underway.

ACKNOWLEDGMENTS

This work has been supported by the National Science Foundation (NSF) under Grants No. PHY1314463, No. ECCS1307378, and No. PHYIIA126117. We would like to thank B. Tregoning and D. Kidd for their valuable help.

[1] O.-A. Al-Hujaj and P. Schmelcher, Phys. Rev. A **70**, 033411 (2004).
[2] J. Mitroy, S. Bubin, W. Horiuchi, Y. Suzuki, L. Adamowicz, W. Cencek, K. Szalewicz, J. Komasa, D. Blume, and K. Varga, Rev. Mod. Phys. **85**, 693 (2013).
[3] Y. Suzuki and K. Varga, *Stochastic Variational Approach to Quantum-Mechanical Few-Body Problems* (Springer, Berlin, 1998).
[4] Y. Tang, L. Wang, X. Song, X. Wang, Z.-C. Yan, and H. Qiao, Phys. Rev. A **87**, 042518 (2013).
[5] A. V. Turbiner and J. C. Lopez Vieyra, Phys. Rev. Lett. **111**, 163003 (2013).
[6] M. Hesse and D. Baye, J. Phys. B **37**, 3937 (2004).
[7] S. Boblest, C. Schimeczek, and G. Wunner, Phys. Rev. A **89**, 012505 (2014).
[8] C. Schimeczek, S. Boblest, D. Meyer, and G. Wunner, Phys. Rev. A **88**, 012509 (2013).
[9] C. Schimeczek and G. Wunner, Comput. Phys. Commun. **185**, 614 (2014).
[10] A. Thirumalai and J. S. Heyl, Phys. Rev. A **89**, 052522 (2014).
[11] J. Avron, I. Herbst, and B. Simon, Phys. Rev. Lett. **39**, 1068 (1977).
[12] J. Avron, I. Herbst, and B. Simon, Commun. Math. Phys. **79**, 529 (1981).
[13] R. Cohen, J. Lodenquai, and M. Ruderman, Phys. Rev. Lett. **25**, 467 (1970).
[14] R. G. Newton, Phys. Rev. D **3**, 626 (1971).
[15] D. H. Constantinescu and P. Rehák, Phys. Rev. D **8**, 1693 (1973).
[16] J. C. Kemp, J. B. Swedlund, J. D. Landstreet, and J. R. P. Angel, Astrophys. J. Lett. **161**, L77 (1970).
[17] J. R. P. Angel, E. F. Borra, and J. D. Landstreet, Astrophys. J. **45**, 457 (1981).
[18] J. Truemper, W. Pietsch, C. Reppin, W. Voges, R. Staubert, and E. Kendziorra, Astrophys. J. Lett. **219**, L105 (1978).
[19] C. Thompson and R. C. Duncan, Astrophys. J. **473**, 322 (1996).
[20] R. C. Ashoori, Nature (London) **379**, 413 (1996).
[21] V. G. Bezchastnov, P. Schmelcher, and L. S. Cederbaum, Phys. Rev. A **75**, 052507 (2007).
[22] V. G. Bezchastnov, P. Schmelcher, and L. S. Cederbaum, Phys. Rev. A **65**, 042512 (2002).
[23] V. G. Bezchastnov, L. S. Cederbaum, and P. Schmelcher, Phys. Rev. A **65**, 032501 (2002).
[24] V. G. Bezchastnov, P. Schmelcher, and L. S. Cederbaum, Phys. Rev. Lett. **95**, 113002 (2005).

[25] V. G. Bezchastnov, L. S. Cederbaum, and P. Schmelcher, Phys. Rev. Lett. **86**, 5450 (2001).
[26] V. G. Bezchastnov, P. Schmelcher, and L. S. Cederbaum, Phys. Rev. A **61**, 052512 (2000).
[27] V. G. Bezchastnov, P. Schmelcher, and L. S. Cederbaum, Phys. Chem. Chem. Phys. **5**, 4981 (2003).
[28] C. F. Bunge and A. V. Bunge, Int. J. Quantum Chem. **14**, 345 (1978).
[29] V. S. Popov and B. M. Karnakov, Phys. Usp. **57**, 257 (2014).
[30] M. V. Ivanov and P. Schmelcher, Phys. Rev. A **57**, 3793 (1998).
[31] W. Becken and P. Schmelcher, Phys. Rev. A **63**, 053412 (2001).
[32] W. Becken and P. Schmelcher, Phys. Rev. A **65**, 033416 (2002).
[33] O.-A. Al-Hujaj and P. Schmelcher, Phys. Rev. A **67**, 023403 (2003).
[34] O.-A. Al-Hujaj and P. Schmelcher, Phys. Rev. A **68**, 053403 (2003).
[35] O.-A. Al-Hujaj and P. Schmelcher, Phys. Rev. A **70**, 023411 (2004).
[36] M. V. Ivanov and P. Schmelcher, Eur. Phys. J. D **14**, 279 (2001).
[37] A. Thirumalai, S. J. Desch, and P. Young, Phys. Rev. A **90**, 052501 (2014).
[38] M. V. Ivanov and P. Schmelcher, Phys. Rev. A **61**, 022505 (2000).
[39] P. Proschel, W. Rosner, G. Wunner, H. Ruder, and H. Herold, J. Phys. B **15**, 1959 (1982).
[40] J. A. Salas and K. Varga, Phys. Rev. A **89**, 052501 (2014).
[41] X. Wang and H. Qiao, Few Body Syst. **53**, 453 (2012).
[42] X. Guan, B. Li, and K. T. Taylor, J. Phys. B **36**, 2465 (2003).
[43] C. A. Nicolaides, Y. Komninos, and D. R. Beck, Phys. Rev. A **24**, 1103 (1981).
[44] K. T. Chung, Phys. Rev. A **20**, 724 (1979).
[45] X. Guan, B. Li, and L. Wu, Phys. Rev. A **64**, 043402 (2001).
[46] J. S. Heyl and L. Hernquist, Phys. Rev. A **58**, 3567 (1998).
[47] H. Qiao and B. Li, Phys. Rev. A **62**, 033401 (2000).
[48] X. Wang and H. Qiao, Phys. Rev. A **75**, 033421 (2007).
[49] E. I. Tellgren, A. M. Teale, J. W. Furness, K. K. Lange, U. Ekström, and T. Helgaker, J. Chem. Phys. **140**, 034101 (2014).
[50] E. I. Tellgren and H. Fliegl, J. Chem. Phys. **139**, 164118 (2013).
[51] E. I. Tellgren, A. Soncini, and T. Helgaker, J. Chem. Phys. **129**, 154114 (2008).
[52] K. K. Lange, E. I. Tellgren, M. R. Hoffmann, and T. Helgaker, Science **337**, 327 (2012).
[53] E. I. Tellgren, S. S. Reine, and T. Helgaker, Phys. Chem. Chem. Phys. **14**, 9492 (2012).
[54] E. I. Tellgren, T. Helgaker, and A. Soncini, Phys. Chem. Chem. Phys. **11**, 5489 (2009).
[55] S. Reimann, U. Ekström, S. Stopkowicz, A. M. Teale, A. Borgoo, and T. Helgaker, Phys. Chem. Chem. Phys. **17**, 18834 (2015).
[56] R. D. Reynolds and T. Shiozaki, Phys. Chem. Chem. Phys. **17**, 14280 (2015).
[57] H. Medel Cobaxin and A. Alijah, J. Phys. Chem. A **117**, 9871 (2013).
[58] Y. P. Kravchenko and M. A. Liberman, Phys. Rev. A **57**, 3403 (1998).
[59] D. Baye and M. Vincke, Phys. Rev. A **42**, 391 (1990).
[60] G. Vignale and M. Rasolt, Phys. Rev. Lett. **59**, 2360 (1987).
[61] M. D. Jones, G. Ortiz, and D. M. Ceperley, Phys. Rev. A **54**, 219 (1996).
[62] Z. Medin and D. Lai, Phys. Rev. A **74**, 062507 (2006).
[63] W. Zhu, L. Zhang, and S. B. Trickey, Phys. Rev. A **90**, 022504 (2014).
[64] A. Thirumalai and J. S. Heyl, Adv. At. Mol. Opt. Phys. **63**, 323 (2014).
[65] S. Bubin, O. V. Prezhdo, and K. Varga, Phys. Rev. A **87**, 054501 (2013).
[66] E. Armour, J.-M. Richard, and K. Varga, Phys. Rep. **413**, 1 (2005).
[67] X. Guan and B. Li, Phys. Rev. A **63**, 043413 (2001).